Cellular/Molecular

Modulation of $Ca_V2.1$ Channels by the Neuronal Calcium-Binding Protein Visinin-Like Protein-2

Nathan J. Lautermilch, Alexandra P. Few, Todd Scheuer, and William A. Catterall
Department of Pharmacology, University of Washington, Seattle, Washington 98195-7280

$Ca_V2.1$ channels conduct P/Q-type Ca^{2+} currents that are modulated by calmodulin (CaM) and the structurally related Ca^{2+}-binding protein 1 (CaBP1). Visinin-like protein-2 (VILIP-2) is a CaM-related Ca^{2+}-binding protein expressed in the neocortex and hippocampus. Coexpression of $Ca_V2.1$ and VILIP-2 in tsA-201 cells resulted in Ca^{2+} channel modulation distinct from CaM and CaBP1. $Ca_V2.1$ channels with β_{2a} subunits undergo Ca^{2+}-dependent facilitation and inactivation attributable to association of endogenous Ca^{2+}/CaM. VILIP-2 coexpression does not alter facilitation measured in paired-pulse experiments but slows the rate of inactivation to that seen without Ca^{2+}/CaM binding and reduces inactivation of Ca^{2+} currents during trains of repetitive depolarizations. $Ca_V2.1$ channels with β_{1b} subunits have rapid voltage-dependent inactivation, and VILIP-2 has no effect on the rate of inactivation or facilitation of the Ca^{2+} current. In contrast, when Ba^{2+} replaces Ca^{2+} as the charge carrier, VILIP-2 slows inactivation. The effects of VILIP-2 are prevented by deletion of the CaM-binding domain (CBD) in the C terminus of $Ca_V2.1$ channels. However, both the CBD and an upstream IQ-like domain must be deleted to prevent VILIP-2 binding. Our results indicate that VILIP-2 binds to the CBD and IQ-like domains of $Ca_V2.1$ channels like CaM but slows inactivation, which enhances facilitation of $Ca_V2.1$ channels during extended trains of stimuli. Comparison of VILIP-2 effects with those of CaBP1 indicates striking differences in modulation of both facilitation and inactivation. Differential regulation of $Ca_V2.1$ channels by CaM, VILIP-2, CaBP1, and other neurospecific Ca^{2+}-binding proteins is a potentially important determinant of Ca^{2+} entry in neurotransmission.

Key words: **facilitation; inactivation; neuromodulation; voltage clamp; synaptic plasticity; calcium current**

Introduction

P/Q-type Ca^{2+} currents initiate exocytosis of neurotransmitters (Takahashi and Momiyama, 1993; Regehr and Mintz, 1994). Because the efficiency of synaptic transmission is proportional to the third power of the local Ca^{2+} concentration (Dodge and Rahamimoff, 1967; Mintz et al., 1995), small changes in Ca^{2+} influx and residual free Ca^{2+} cause multiple forms of short-term synaptic plasticity that have an important influence on synaptic function (Zucker and Regehr, 2002). $Ca_V2.1$ channels mediate P/Q-type currents (Llinás et al., 1989; Starr et al., 1991; Wheeler et al., 1994), and these channels are localized in high density in presynaptic active zones of central neurons (Westenbroek et al., 1995; Sakurai et al., 1996; Wu et al., 1999).

Ca^{2+} binding to calmodulin (CaM) causes facilitation and enhances inactivation of $Ca_V2.1$ channels through binding to a site in the C-terminal domain (Lee et al., 1999, 2000; Pate et al., 2000; DeMaria et al., 2001). Ca^{2+}-binding protein 1 (CaBP1), a neurospecific CaM-like Ca^{2+} binding protein, accelerates inactivation, prevents facilitation, and binds at the same site as CaM in a Ca^{2+}-independent manner (Lee et al., 2002). These results raise the possibility that multiple CaM-related neuronal CaBPs (nCaBPs) may interact with the C-terminal regulatory site and differentially regulate $Ca_V2.1$ channels.

Visinin-like proteins (VILIPs) belong to the neuronal Ca^{2+} sensor superfamily (Haeseleer et al., 2000; Burgoyne and Weiss, 2001) and are expressed in retinal (Lenz et al., 1992) and brain neurons (Saitoh et al., 1995; Bernstein et al., 1999, 2003; Hamashima et al., 2001; Spilker et al., 2002). They sensitize G-protein signaling cascades to Ca^{2+} and enhance desensitization of G-protein-coupled receptors (De Castro et al., 1995; Ames et al., 1997; Sallese et al., 2000), which can regulate $Ca_V2.1$ channels through $G\beta\gamma$ subunits (Herlitze et al., 1996; Ikeda, 1996). VILIPs reversibly translocate to membranes in response to Ca^{2+} fluctuations in neurons (Spilker et al., 2002), suggesting that they may shuttle between the plasma membrane and intracellular compartments in response to Ca^{2+} channel activity.

The kinetics and voltage dependence of activation and inactivation of Ca^{2+} channels are strongly influenced by their $Ca_V\beta$ subunits (Hofmann et al., 1999; Lee et al., 2000; Arikkath and Campbell, 2003). The β_{1b} subunit causes rapid voltage-dependent inactivation, similar to β_3 and β_4 (De Waard and Campbell, 1995), whereas the β_{2a} subunit slows channel inactivation (Olcese et al., 1994; Chien et al., 1996). The rapid inactivation of $Ca_V2.1$ channels with β_{1b} subunits substantially reduces Ca^{2+}/CaM-dependent facilitation compared with β_{2a} subunits

Received Feb. 2, 2005; revised April 20, 2005; accepted May 14, 2005.

This work was supported by National Institutes of Health Grants R01 NS 22625 (W.A.C.), F32 NS 11099 (N.J.L.), and T32 GM07270 (A.P.F.). We thank Dr. Amy Lee (Emory University, Atlanta, GA) for cDNA constructs and for valuable discussions.

Correspondence should be addressed to William Catterall, Department of Pharmacology, University of Washington School of Medicine, 1959 Northeast Pacific Street, Room F427, Seattle, WA 98195. E-mail: wcatt@u.washington.edu.

N. J. Lautermilch's present address: MDS Pharma Services, 22011 30th Drive Southeast, Bothell, WA 98021-4444.

DOI:10.1523/JNEUROSCI.0447-05.2005

 0270-6474/05/257062-●$15.00/0

(Lee et al., 1999). Both β_{1b} and β_{2a} are coexpressed with $Ca_V2.1$ (Stea et al., 1994; Tanaka et al., 1995; Ludwig et al., 1997; Burgess et al., 1999) and are likely to form functional channels *in vivo*. In this report, we describe modulation of $Ca_V2.1$ channels having β_{1b} or β_{2a} subunits by VILIP-2 and compare these results with modulation by CaBP1. Our results show that VILIP-2 modulates $Ca_V2.1$ channels in a manner distinct from CaM and CaBP1, supporting the conclusion that $Ca_V2.1$ channel properties are fine-tuned by interaction of multiple neuronal Ca^{2+}-binding proteins at a common C-terminal regulatory site.

Materials and Methods

Cloning of VILIP-2. A full-length cDNA clone of VILIP-2 was isolated from total rat brain mRNA. VILIP-2-specific cDNA was generated with reverse primer TCTAGACTACTTCTGCATG using Superscript First-Strand Synthesis system for reverse transcription-PCR (Invitrogen, San Diego, CA). Using the same reverse primer and the forward primer CTCGAGATGGGGAAGAACAATAGC, we amplified a single band that was cloned via the TOPO TA cloning kit (Invitrogen). This was sequence verified and subcloned into pcDNA 3.1+. Construction of a carboxyl myc-tagged form of VILIP-2 (VILIP-2 myc) was accomplished by PCR using the same forward primer and the reverse primer TCTAGACTACAAGTCCTCTTCAGAAATGAGCTTTTGCTCCTTCTGCATG, which was amplified and cloned via TOPO TA cloning kit and subcloned into pcDNA 3.1+. The myc tag was detected with an anti-myc antibody from Invitrogen.

cDNA expression constructs. Expression vectors for rat $Ca_V2.1$ channels were prepared by subcloning wild-type and mutant subunit cDNAs into the following plasmids: $\alpha_1$2.1(rbA-II) in pcDNA 3.1+, $\alpha_1$2.1ΔCBD (CaM-binding domain), $\alpha_1$2.1 1965 stop, $\alpha_1$2.1 IQ-AA, $\alpha_1$2.1 IQ-AA/ΔCBD in pMT2, β_{1b} and β_{2a} in pMT2XS, and $\alpha_2\delta$ in pZEM228 (Ellis et al., 1988; Starr et al., 1991; Perez-Reyes et al., 1992; Stea et al., 1994), as described previously (Lee et al., 1999, 2000, 2003). CaBP1 constructs were prepared as described previously (Lee et al., 2002).

Cell culture and transfection. tsA-201 cells were maintained in DMEM/F-12 supplemented with 10% fetal bovine serum (Invitrogen) at 37°C under 10% CO_2. Cells plated in 35 mm culture dishes for electrophysiological recording were grown to 70% confluence and transfected by the $CaPO_4$ method with a total of 5 μg of DNA, including a 1:1 molar ratio of Ca^{2+} channel subunits ($\alpha_1$2.1, β_{1b} or β_{2a}, and $\alpha_2\delta$), 0.3 μg of CD8 expression plasmid for identification of transfected cells, and 1 μg of VILIP-2 cDNA. Biochemical studies used 150 mm dishes with a maximum of 70 μg of DNA using the same ratios as above, but without CD8.

Electrophysiology. tsA-201 cells were incubated with CD8 antibody-coated microspheres (Dynal Biotech, Oslo, Norway) to allow visual identification of transfected cells 48–72 h after transfection. Ca^{2+} currents were recorded in the whole-cell configuration of the patch-clamp technique using an Axopatch 200A patch-clamp amplifier (Molecular Devices, Union City, CA) and were filtered at 5 kHz. Voltage protocols were applied with Pulse software (HEKA Elektronik, Lambrecht/Pfalz, Germany), and data were analyzed using IGOR Pro 4.0 software (WaveMetrics, Lake Oswego, OR). Leak and capacitive transients were subtracted using P/−4 protocol. The extracellular recording solution contained the following (in mM): 150 Tris, 1 $MgCl_2$, and 10 $CaCl_2$ or $BaCl_2$, adjusted to pH 7.3 with methanesulfonic acid, except where differences are noted in Figures 1–8. Intracellular solutions contained the following (in mM): 120 *N*-methyl-D-glucamine, 60 HEPES, 1 $MgCl_2$, 2 Mg-ATP, and either 0.5 or 10 EGTA, adjusted to pH 7.3 with methanesulfonic acid. Because extracellular Ba^{2+} caused positive shifts in the voltage dependence of activation of 10 mV, voltage protocols were adjusted to compensate for this difference, as noted in Figures 1–8. All averaged data represent the mean ± SEM. The current traces presented in Figures 1–8 represent the means of normalized current traces from the indicated number of samples for each experimental condition.

Biochemical studies. tsA-201 cells were cultured and transfected as described above and harvested 48 h after transfection. Dithiobis (succinimidyl propionate) (DSP; 2 mM; Pierce, Rockford, IL) was dissolved in DMSO and applied for 30 min in PBS, followed by quenching in Tris. Cells were harvested in lysis buffer containing 150 mM NaCl, 10 mM EGTA, 20 mM TrisHCl, and 1% NP-40. Lysates were passed through a syringe needle (3 ml of 25G 5/8) four times, followed by centrifugation at 14,000 rpm for 10 min to remove the nuclear fraction. Anti-CNA4 (10 μg) directed against $\alpha_1$2.1 (Sakurai et al., 1996) or IgG control antibody was incubated for 1 h, followed by 15 min protein A-Sepharose bead precipitation. Beads were washed three times in lysis buffer with 0.1% NP-40, heated to 95°C for 10 min in loading buffer containing 0.1 M DTT, and separated by SDS-PAGE in a 4–20% acrylamide gel. Proteins were transferred onto nitrocellulose membranes, blocked in 3% nonfat milk and 0.5% SDS for 2 h, and probed with either anti-CNA4 (1:100) or anti-myc (1:5000), followed by secondary labeling with horseradish peroxidase-linked protein A (Amersham Biosciences, Piscatway, NJ) or horseradish peroxidase-linked sheep anti-mouse (Amersham Biosciences). Bound horseradish peroxidase was detected by ECL reaction (Amersham Biosciences) followed by exposure to film.

Results

Coexpression of VILIP-2 with $Ca_V2.1/\beta_{2a}$ channels

We first examined the effect of coexpression of VILIP-2 on Ca^{2+} currents (I_{Ca}) in whole-cell voltage-clamp recordings of transfected tsA-201 cells expressing $Ca_V2.1$ channels with β_{2a} subunits. Ca^{2+} currents were observed in test pulses to potentials more positive than −10 mV, approached maximum at +40 mV, and inactivated slowly during long pulses (Fig. 1*A*,*B*, gray). Coexpression of VILIP-2 did not affect the voltage dependence of activation of $Ca_V2.1$ channels in response to depolarizing test pulses to different membrane potentials (Fig. 1*A*, black). I_{Ca} inactivates ~53% during a 1 s test pulse (Fig. 1*B*, gray) compared with 31% for Ba^{2+} current (I_{Ba}) (Fig. 1*C*, gray). This Ca^{2+}-dependent component of inactivation is caused by endogenous CaM, which binds entering Ca^{2+} and interacts with the CBD in the C terminus to inactivate $Ca_V2.1$ channels (Lee et al., 1999, 2003). When VILIP-2 is coexpressed with $Ca_V2.1/\beta_{2a}$ channels, the rate of inactivation of I_{Ca} is slowed considerably (Fig. 1*B*, black). In contrast to I_{Ca}, VILIP-2 has no effect on the rate of inactivation of I_{Ba} conducted by $Ca_V2.1/\beta_{2a}$ channels (Fig. 1*C*). The block of Ca^{2+}-dependent inactivation by VILIP-2 suggests that it may prevent binding of endogenous Ca^{2+}/CaM to the CBD of $Ca_V2.1$ channels.

A deletion mutant of $Ca_V2.1$ lacking the CBD ($Ca_V2.1\Delta CBD$) conducts Ca^{2+} currents that do not undergo rapid CaM-dependent inactivation (Fig. 1*D*, gray), confirming that CaM association with the CBD is required for Ca^{2+}-dependent inactivation. Expression of VILIP-2 with $Ca_V2.1\Delta CBD$ has no effect on its inactivation (Fig. 1*D*, black), supporting the conclusion that VILIP-2 acts primarily to negate the effect of endogenous Ca^{2+}/CaM on $Ca_V2.1/\beta_{2a}$ channels. Because VILIP-2 has no effect on inactivation of the $Ca_V2.1\Delta CBD$ channel, either VILIP-2 does not bind to $Ca_V2.1\Delta CBD$ or it binds but has no effect on inactivation.

Coexpression of VILIP-2 with $Ca_V2.1/\beta_{1b}$ channels

When $Ca_V2.1$ is coexpressed with the β_{1b} subunit, voltage-dependent inactivation of I_{Ca} is faster than for $Ca_V2.1/\beta_{2a}$ (Fig. 1, compare *E*, gray with *B*, gray), and it is unaffected by coexpression of VILIP-2 (Fig. 1*E*, black). Inactivation of I_{Ba} conducted by $Ca_V2.1/\beta_{1b}$ is also more rapid than inactivation of I_{Ba} of $Ca_V2.1/\beta_{2a}$ channels (Fig. 1, compare *F*, gray with *C*, gray), and it is substantially slowed by coexpression of VILIP-2 (Fig. 1*F*, black), without effect on the voltage dependence of activation (data not shown). In contrast, the $Ca_V2.1\Delta CBD/\beta_{1b}$ mutant channel is unaffected by VILIP-2 (Fig. 1*G*), indicating that VILIP-2 acts at the same site as CaM to control the rate of inactivation. Because

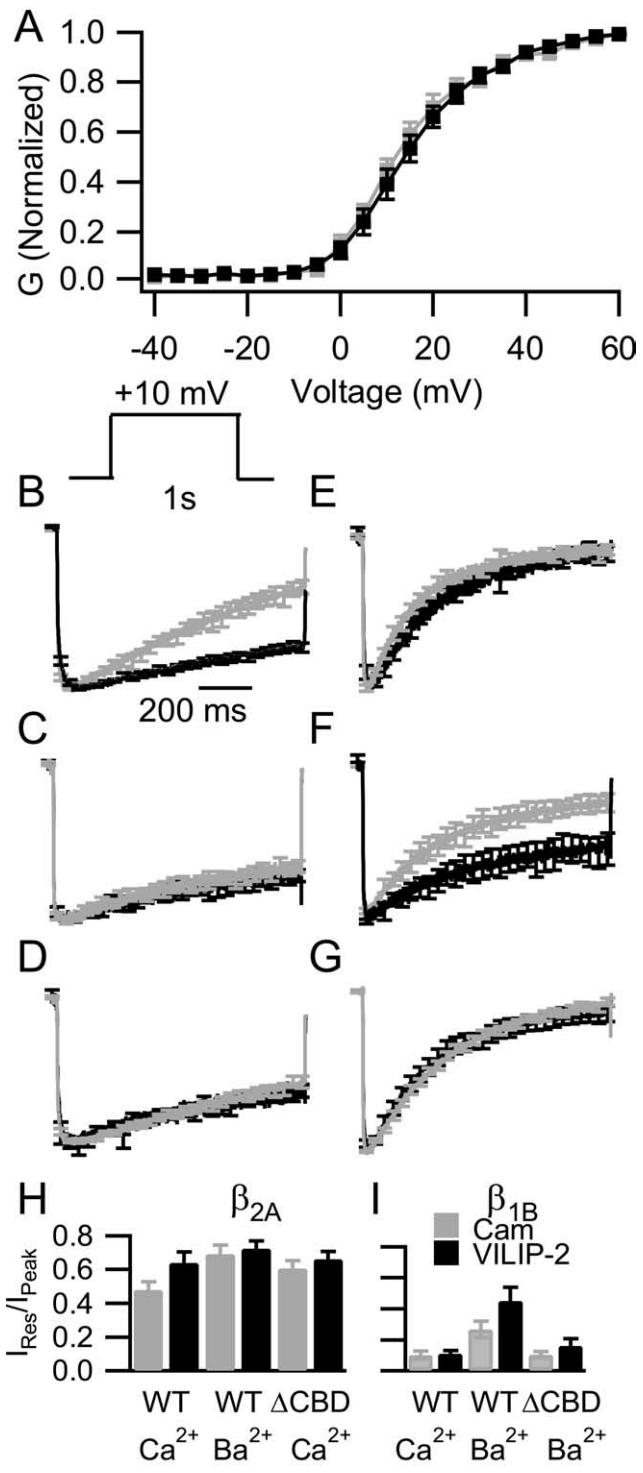

Figure 1. Effect of coexpression of VILIP-2 on $Ca_V2.1$ channels. ***A***, Voltage dependence of activation. $Ca_V2.1/\beta_{2a}$ channels was activated by 5 ms pulses to the indicated potentials from a holding potential of −80 mV, and Ca^{2+} tail currents were recorded after repolarization to −40 mV without (gray) or with (black) coexpression of VILIP-2 (±SEM; $n \geq 10$). ***B***, I_{Ca} was evoked by 1 s depolarizing test pulses to +10 mV from a holding potential of −80 mV in tsA-201 cells expressing $Ca_V2.1/\beta_{2a}$ channels without (gray) or with (black) VILIP-2. Current records were normalized to the peak inward current and averaged (±SEM; $n \geq 10$). ***C***, I_{Ba} was evoked and analyzed as in ***B***. ***D***, I_{Ca} was evoked and analyzed as in ***B*** for $Ca_V2.1\Delta CBD/\beta_{2a}$. ***E***, I_{Ca} conducted by $Ca_V2.1/\beta_{1b}$ channels was evoked and analyzed as in ***B***. ***F***, I_{Ba} conducted by $Ca_V2.1/\beta_{1b}$ channels was evoked and analyzed as in ***B***. ***G***, I_{Ba} conducted by $Ca_V2.1\Delta CBD/\beta_{1b}$ channels was evoked and analyzed as in ***B***. ***H***, ***I***, Residual current amplitude at the end of the 1 s pulse (I_{Res}) was divided by peak current from cells transfected with $Ca_V2.1$ alone (gray) or with VILIP-2 (black) for the indicated experimental conditions. WT, Wild type. Error bars represent SEM.

VILIP-2 alters the rate of inactivation of I_{Ba}, it must associate with $Ca_V2.1$ channels at the resting level of intracellular Ca^{2+} and slow voltage-dependent inactivation. However, although VILIP-2 is bound to the $Ca_V2.1/\beta_{1b}$ channel, it is unable to slow the inactivation of I_{Ca} appreciably, presumably because of the strong driving force for inactivation with both β_{1b} and Ca^{2+} bound to the channel complex. Overall, VILIP-2 appears to act by negating rapid Ca^{2+}/CaM-dependent inactivation and slowing voltage-dependent inactivation in a β subunit-dependent manner.

Paired-pulse facilitation of $Ca_V2.1/\beta_{2a}$ channels coexpressed with VILIP-2

I_{Ca} conducted by $Ca_V2.1/\beta_{2a}$ channels is significantly facilitated after a previous depolarizing pulse, resulting from Ca^{2+}/CaM interaction with the IQ-like domain and CBD (Lee et al., 2000, 2003; DeMaria et al., 2001). With 10 mM EGTA in the recording pipette, Ca^{2+} facilitation can be recorded in isolation without interference from Ca^{2+}-dependent inactivation (Lee et al., 2000). Applying a similar protocol, we found that paired-pulse facilitation of I_{Ca} was unchanged by coexpression of VILIP-2 (Fig. 2*A*). As expected, no facilitation of I_{Ba} was observed without or with VILIP-2 (Fig. 2*B*). Evidently, although VILIP-2 modulates inactivation differently from CaM, it can mediate Ca^{2+}-dependent paired-pulse facilitation similarly.

Ca^{2+}-dependent facilitation and inactivation during trains of depolarizations

Previous work demonstrated that activity-dependent increases in Ca^{2+} entry cause facilitation attributable to a local increase in Ca^{2+}, followed by inactivation attributable to a more global increase in Ca^{2+} during extended trains of depolarizations (Lee et al., 2000). These trains of brief depolarizations more closely resemble electrical activity in nerve terminals than single long depolarizing pulses. This dual regulation is caused by stepwise Ca^{2+} binding to C- and N-terminal lobes of CaM and sequential binding of Ca^{2+}/CaM to the IQ-like domain and CBD of $Ca_V2.1$ channels (Lee et al., 1999, 2000, 2003; DeMaria et al., 2001). To investigate the effects of VILIP-2 coexpression on $Ca_V2.1$ channels during trains of brief stimuli, we depolarized tsA-201 cells expressing $Ca_V2.1/\beta_{2a}$ channels repetitively to +10 mV for 5 ms at a frequency of 100 Hz and recorded I_{Ca} during each stimulation. Initially, we observed that VILIP-2 prevented both facilitation and subsequent inactivation (data not shown). However, on more careful analysis, we realized that the residual increase in Ca^{2+} concentration from previous depolarization protocols was occluding facilitation. By recording from cells that either had not experienced stimulated Ca^{2+} influx or were allowed to recover from previous depolarizations for at least 2 min, we were able to accurately record both facilitation and inactivation by CaM (Fig. 3*A*,*C*, gray) and facilitation by VILIP-2 (Fig. 3*B*,*C*, black). VILIP-2 coexpression increased the amount of facilitation and decreased the rate of pulse-wise inactivation of I_{Ca} compared with control cells not expressing VILIP-2 (Fig. 3*C*). As expected from the lack of effect of VILIP-2 on paired-pulse facilitation, it had insignificant effects during the first few pulses but reduced the pulse-wise inactivation of I_{Ca} thereafter. In contrast, when Ba^{2+} replaced Ca^{2+} as the charge carrier, insignificant facilitation was observed with endogenous CaM in control cells or after coexpression of VILIP-2 (Fig. 3*E*). These results are in agreement with our observation (Fig. 1) that VILIP-2 slows the rate of Ca^{2+}-dependent inactivation of $Ca_V2.1/\beta_{2a}$ channels during single long depolarizations and show further that VILIP-2 enhances facilitation during extended trains of stimuli in a Ca^{2+}-dependent man-

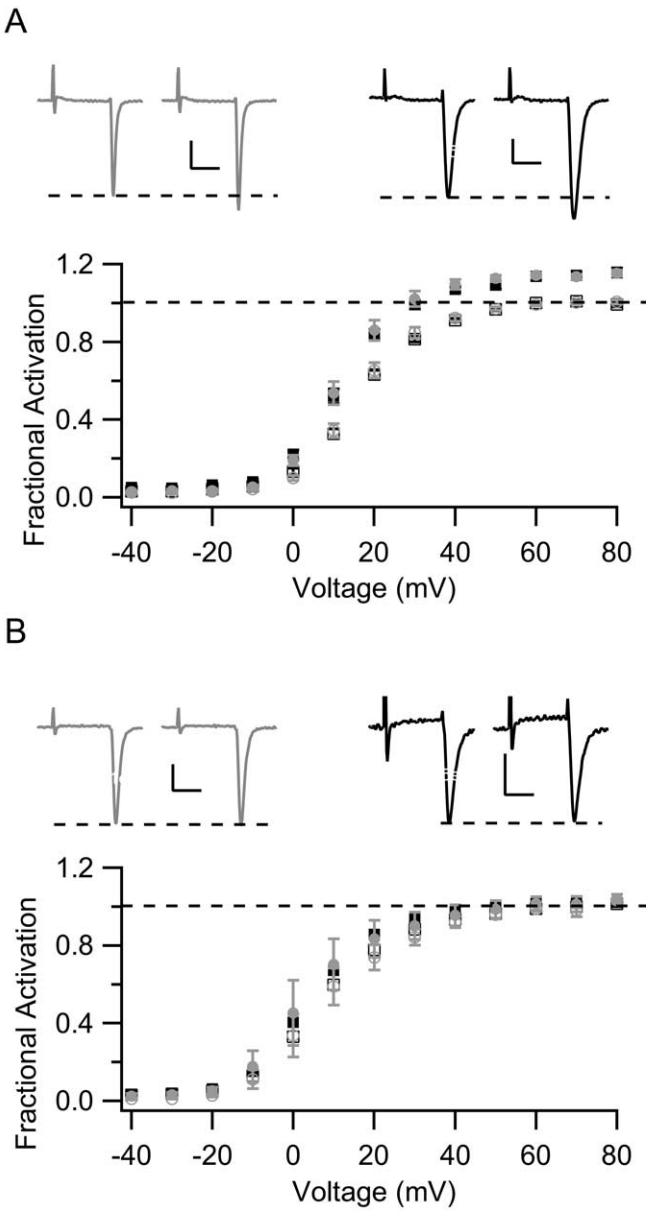

Figure 2. Effect of coexpression of VILIP-2 on paired-pulse facilitation of $Ca_V2.1/\beta_{2a}$ channels. Test pulses to potentials ranging from −40 to +80 mV were applied without a prepulse (open symbols) or with a 50 ms prepulse to +10 mV and an 8 ms period at −80 mV before the test pulse (filled symbols). ***A***, Peak inward calcium currents for cells expressing $Ca_V2.1/\beta_{2a}$ channels without (gray circles) or with (black squares) VILIP-2. ***B***, Same protocol as that in ***A***, with 10 mM barium as the charge carrier. Insets, Representative calcium or barium currents at 70 mV. Calibration: horizontal, 2 ms; vertical, ***A***, ***B***, left insets, 1 nA; ***A***, ***B***, right insets, 500 pA. Error bars represent SEM.

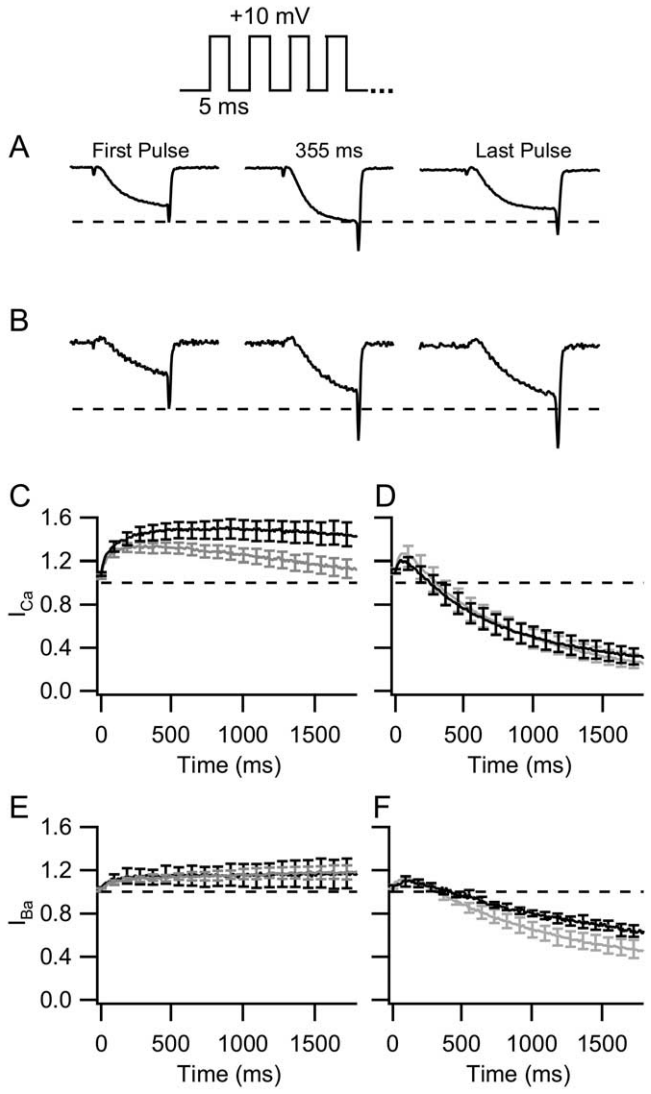

Figure 3. Effect of VILIP-2 on facilitation and inactivation of $Ca_V2.1$ channels during trains of repetitive depolarizations. Test pulses to +10 mV (0 mV for I_{Ba}) for 5 ms at a frequency of 100 Hz were applied to transfected tsA-201 cells expressing $Ca_V2.1$ channels only (gray) or $Ca_V2.1$ channels plus VILIP-2 (black). Peak current amplitudes were normalized to the first pulse in the series and plotted against time (±SEM; $n \geq 10$; every 10th SEM is plotted). ***A***, Representative I_{Ca} measured for the first pulse, the pulse at 355 ms, and the last pulse in a train of stimuli for $Ca_V2.1/\beta_{2a}$ alone. ***B***, Representative I_{Ca} measured for the first pulse, the pulse at 355 ms, and the last pulse in a train of stimuli for $Ca_V2.1/\beta_{2a}$ plus VILIP-2. ***C***, I_{Ca}, $Ca_V2.1/\beta_{2a}$. ***D***, I_{Ca}, $Ca_V2.1/\beta_{1b}$. ***E***, I_{Ba}, $Ca_V2.1/\beta_{2a}$. ***F***, I_{Ba}, $Ca_V2.1/\beta_{1b}$. Error bars represent SEM.

ner. Because VILIP-2 has no effect on facilitation by a single pulse, it is likely that the increase in facilitation during trains of stimuli reflects slowing of cumulative Ca^{2+}-dependent inactivation.

When the β_{1b} subunit was coexpressed with $Ca_V2.1$, and Ca^{2+} was the charge carrier, trains of stimuli elicited brief facilitation followed by rapid, pulse-wise inactivation (Fig. 3*D*, gray). VILIP-2 had no effect on facilitation or inactivation of I_{Ca} during repetitive depolarizations (Fig. 3*D*, black). However, when Ba^{2+} replaced Ca^{2+} as the charge carrier, minimal facilitation of the current was observed, and inactivation was reduced. Coexpression of VILIP-2 reduced the rate of the remaining pulse-wise inactivation (Fig. 3*F*, black) compared with control cells (Fig. 3*F*, gray), similar to the reduced inactivation of I_{Ba} we observed during single long depolarizations (Fig. 1*F*). The effects of VILIP-2 on facilitation and inactivation of both $Ca_V2.1/\beta_{2a}$ channels and $Ca_V2.1/\beta_{1b}$ channels are consistent with a model in which VILIP-2 associates with the CBD at resting levels of Ca^{2+}, blocks the effects of CaM, slows inactivation, and thereby enhances facilitation in a β subunit-dependent manner.

Modulation of $Ca_V2.1$ channels by VILIP-2 after trains of depolarizations

To further characterize the effects of trains of depolarizations on the modulation of $Ca_V2.1$ channels by VILIP-2, we used a double-pulse protocol in which a 1 s depolarizing test pulse was followed by a 600 ms train of depolarizations to +20 mV for 5 ms at 100 Hz and finally by a second identical test pulse. This proto-

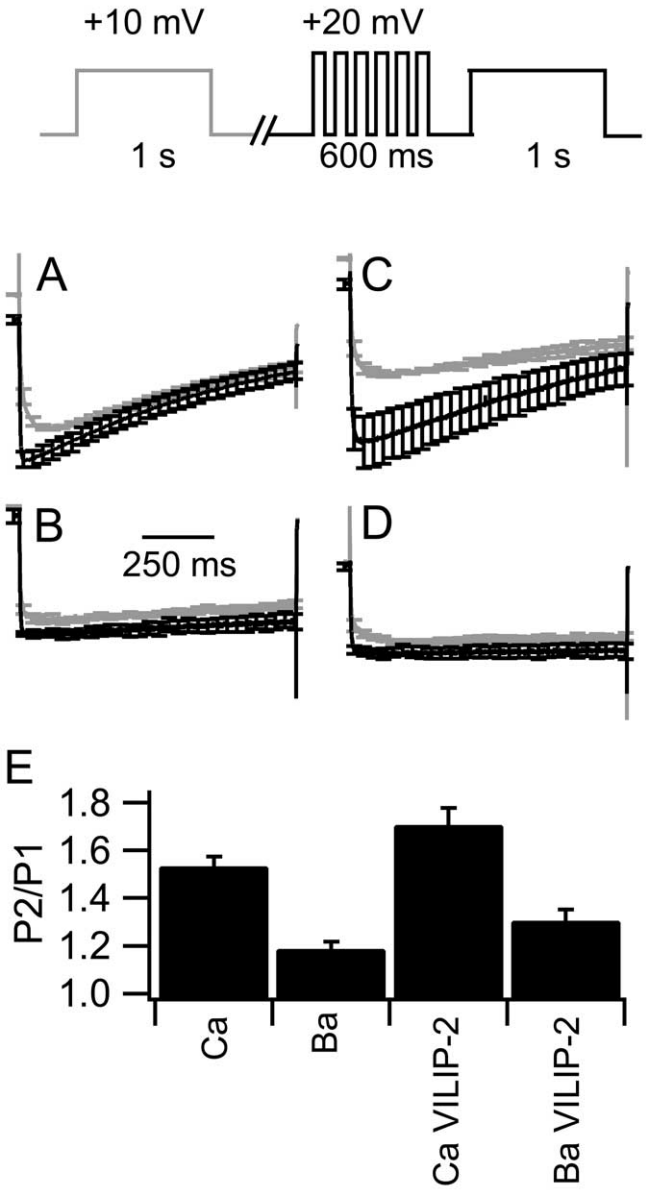

Figure 4. Effect of VILIP-2 on $Ca_V2.1/\beta_{2a}$ channels after trains of repetitive depolarizations. $Ca_V2.1/\beta_{2a}$ channel currents were evoked by 1 s test pulses to +10 mV before (gray) or after (black) a 600 ms train of 5 ms depolarizations to +20 mV (+10 mV for I_{Ba}) at 100 Hz. A 2 min interval was maintained between applications of this protocol to allow the effects of the previous stimuli to return to baseline. Current amplitudes were normalized to the peak current of the first test pulse. Mean normalized currents during test pulse 1 (gray) and test pulse 2 (black) are overlaid. ***A***, I_{Ca}, $Ca_V2.1/\beta_{2a}$ alone. ***B***, I_{Ba}, $Ca_V2.1/\beta_{2a}$ alone. ***C***, I_{Ca}, $Ca_V2.1/\beta_{2a}$ plus VILIP-2. ***D***, I_{Ba}, $Ca_V2.1/\beta_{2a}$ plus VILIP-2. ***E***, Bar graph presenting facilitation as the pulse ratio (P2/P1) at the time of the peak current in each panel (mean ± SEM). Error bars represent SEM.

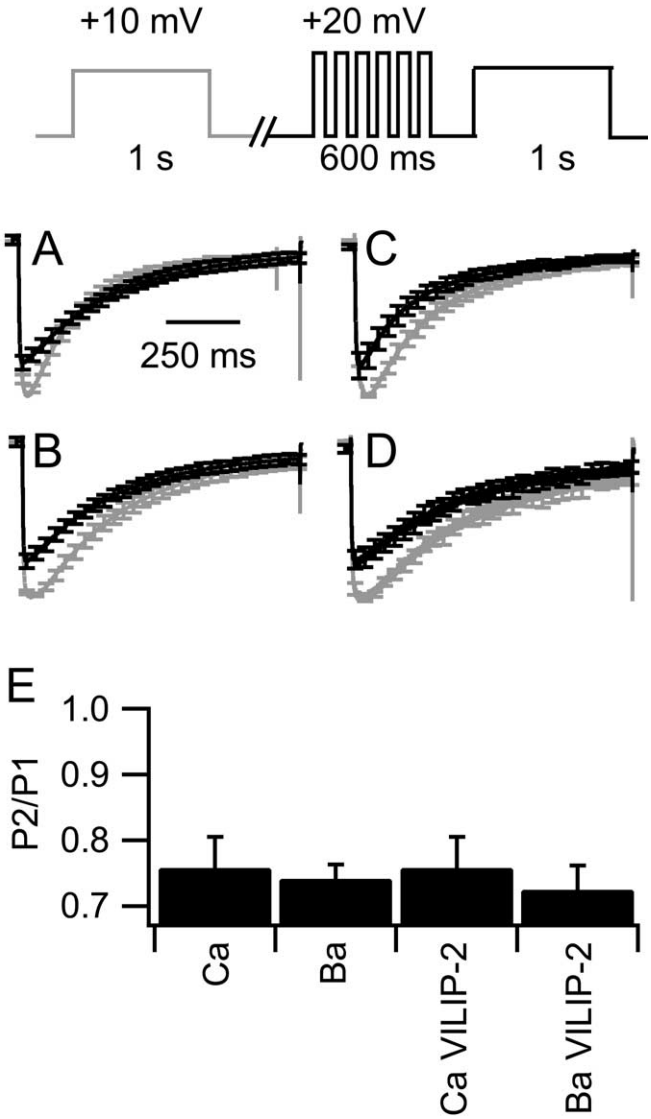

Figure 5. Effect of VILIP-2 on $Ca_V2.1/\beta_{1b}$ channels after trains of repetitive depolarizations. $Ca_V2.1/\beta_{1b}$ channel currents were evoked by 1 s test pulses to +10 mV before (gray) or after (black) a 600 ms train of repetitive depolarization to +20 mV (+10 mV for I_{Ba}) for 5 ms at 100 Hz. A 2 min interval was maintained between applications of this protocol to allow the effects of the previous stimuli to return to baseline. Current amplitudes were normalized to the peak current of the first test pulse. Mean normalized currents during test pulse 1 (gray) and test pulse 2 (black) are overlaid. ***A***, I_{Ca}, $Ca_V2.1/\beta_{1b}$ alone. ***B***, I_{Ba}, $Ca_V2.1/\beta_{1b}$ alone. ***C***, I_{Ca}, $Ca_V2.1/\beta_{1b}$ plus VILIP-2. ***D***, I_{Ba}, $Ca_V2.1/\beta_{1b}$ plus VILIP-2. ***E***, Bar graph presenting facilitation as the pulse ratio (P2/P1) at the time of the peak current in each panel (mean ± SEM). Error bars represent SEM.

col is expected to cause accumulation of Ca^{2+} in the vicinity of Ca^{2+} channels during the train of depolarizations, which will modulate the activation and inactivation of the $Ca_V2.1$ channels in the second test pulse compared with the first. For $Ca_V2.1$ channels containing the β_{2a} subunit, the rate of activation and the peak amplitude of I_{Ca} during 1 s test pulses to +10 mV are significantly increased after the pulse train (Fig. 4*A*, black, *E*) compared with before the train of stimuli (Fig. 4*A*, gray, *E*). These effects are not observed for I_{Ba}, indicating that they are caused by Ca^{2+} entering the cells during the train of stimuli (Fig. 4*B*,*E*). For cells coexpressing VILIP-2, the peak amplitude of I_{Ca} is further enhanced after the train of depolarizing stimuli (Fig. 4*C*), and this effect is also lost when Ba^{2+} is the current carrier (Fig. 4*D*,*E*). Thus, VILIP-2 increases the Ca^{2+}-dependent facilitation of I_{Ca} conducted by $Ca_V2.1/\beta_{2a}$ channels after a train of depolarizations, as observed in the experiments shown in Figure 2 for I_{Ca} recorded during the brief depolarizations within the train. As for depolarizations within the train, it is likely that the enhanced facilitation caused by VILIP-2 reflects slowing of cumulative inactivation of I_{Ca} during the pulse train.

We next examined the effect of a train of repetitive depolarizing stimuli on $Ca_V2.1$ channels containing the β_{1b} subunit (Fig. 5). In contrast to $Ca_V2.1/\beta_{2a}$ channels, previous stimulation of $Ca_V2.1/\beta_{1b}$ channels with a train of depolarizing pulses reduces peak I_{Ca} (Fig. 5*A*, black) compared with currents recorded during

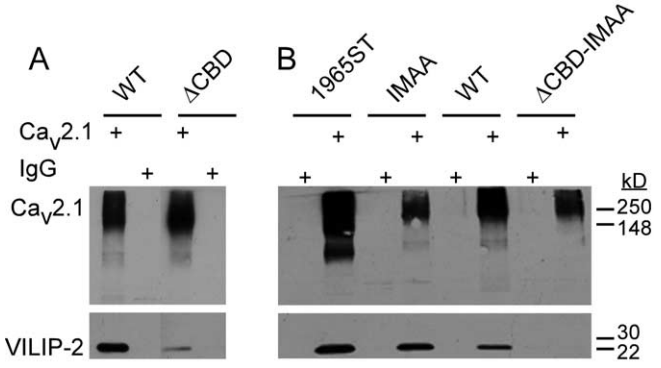

Figure 6. Association of VILIP-2 with $Ca_V2.1$ channels via the IQ-like domain and CBD. Transfected cells were cross-linked *in situ* with DSP, as described in Materials and Methods. ***A***, Lysates from cells transfected with $Ca_V2.1$ plus VILIP-2 myc or $Ca_V2.1\Delta$CBD plus VILIP-2 myc were subjected to immunoprecipitation by anti-$Ca_V2.1$ antibodies or control IgG as indicated in the presence of 10 mM EGTA. ***B***, Lysates from cells transfected with $Ca_V2.1$, $Ca_V2.1$/1965ST, $Ca_V2.1$/IM-AA, and $Ca_V2.1\Delta$CBD/IM-AA plus VILIP-2 myc were subjected to immunoprecipitation by anti-$Ca_V2.1$ antibodies or control IgG in the presence of 10 mM EGTA. Blots were probed with either anti-$Ca_V2.1$ (top) or anti-myc (bottom). WT, Wild type.

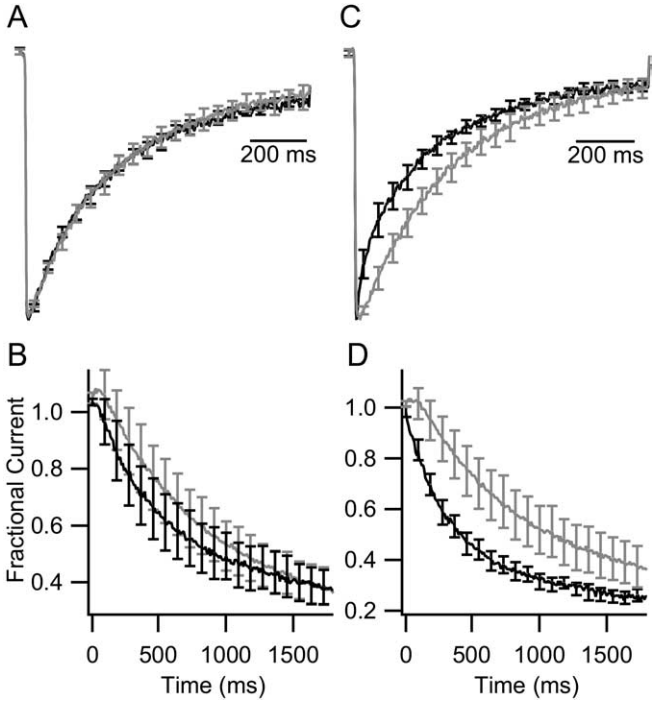

Figure 7. Effect of CaBP1 on $Ca_V2.1/\beta_{1b}$ channels. ***A***, Average, smoothed I_{Ca} conducted by $Ca_V2.1$ channels evoked by 1 s depolarizing pulses from a holding potential of −80 mV to +30 mV without (gray) or with (black) coexpression of CaBP1 (±SEM; $n = 5–7$). ***B***, From a holding potential of −80 mV, test pulses to +10 mV for 5 ms at a frequency of 100 Hz were applied to transfected tsA-201 cells expressing $Ca_V2.1$ channels alone (gray) or $Ca_V2.1$ channels plus CaBP1 (black). Peak current amplitudes were normalized to the first pulse in the series and plotted against time of stimulation (±SEM; $n = 8–10$; every 10th SEM is plotted). ***C***, Averaged, smoothed I_{Ba} was measured as in ***A*** with a test pulse to +20 mV for $Ca_V2.1/\beta_{1b}$ channels without (gray) or with (black) coexpression of CaBP1 (±SEM; $n = 5–8$). ***D***, From a holding potential of −80 mV, test pulses to 0 mV for 5 ms at a frequency of 100 Hz were applied to transfected tsA-201 cells expressing $Ca_V2.1/\beta_{1b}$ channels without (gray) or with (black) coexpression of CaBP1. Peak current amplitudes were normalized to the first pulse in the series and plotted against time (±SEM; $n = 6–8$; every 10th SEM is plotted). Error bars represent SEM.

an identical test pulse immediately before the train (Fig. 5*A*, gray), yielding a pulse ratio [pulse 2 (P2)/P1] significantly <1.0 (Fig. 5*E*). Similar results are obtained for I_{Ba} (Fig. 5*B*), indicating that these effects of the train of prepulses are independent of Ca^{2+} and therefore reflect cumulative voltage-dependent inactivation. Coexpression of VILIP-2 has little effect on the response of I_{Ba} conducted by $Ca_V2.1/\beta_{1b}$ channels to a train of depolarizations (Fig. 5*C*,*D*). Evidently, the effects of VILIP-2 on facilitation and inactivation after trains of prepulses are specific for $Ca_V2.1$ channels containing β_{2a} subunits, which have substantial Ca^{2+}-dependent facilitation and inactivation.

Association of VILIP-2 with $Ca_V2.1$ channels

We measured the association of VILIP-2 and $Ca_V2.1$ channels in coimmunoprecipitation studies by coexpressing a myc-tagged form of VILIP-2 with $Ca_V2.1$ and the β_{1b} subunit. Our initial experiments failed to demonstrate interaction of VILIP-2 with $Ca_V2.1$ channels after detergent solubilization and immunoprecipitation, indicating that the complex formed is reversible and dissociates during isolation. In contrast to these results, *in situ* protein cross-linking with DSP applied to intact cells (see Materials and Methods), followed by detergent extraction and immunoprecipitation, resulted in detection of VILIP-2 binding to $Ca_V2.1$ channels at resting levels of Ca^{2+} (Fig. 6*A*, WT). Coimmunoprecipitation of VILIP-2 was specific, because VILIP-2 was not coimmunoprecipitated with control IgG in cells transfected with $Ca_V2.1$ and VILIP-2.

CaM binds to two closely spaced motifs in the C terminus of $Ca_V2.1$ channels, the CBD and the IQ-like domain (Lee et al., 1999, 2000, 2003; DeMaria et al., 2001; Erickson et al., 2003). Deletion of the CBD or deletion of the carboxyl-half of the C terminus containing the CBD at amino acid 1965 caused a variable decrease in VILIP-2 binding (Fig. 6*A*, ΔCBD, *B*, 1965ST), suggesting that VILIP-2 bound to a second site or subsite in addition to the CBD. Mutation of the first two amino acid residues of the IQ-like domain had little effect on binding of VILIP-2 (Fig. 6*B*, IMAA). In contrast, combined mutation of the CBD and the IQ-like domain consistently prevented VILIP-2 binding (Fig. 6*B*, ΔCBD-IMAA). These results indicate that VILIP-2, like CaM (Lee et al., 1999, 2000, 2003; DeMaria et al., 2001; Erickson et al., 2003), binds to both the IQ-like domain and the CBD of $Ca_V2.1$ channels.

Modulation of $Ca_V2.1/\beta_{1b}$ channels by CaBP1

In previous studies, we examined the effects of CaBP1 on $Ca_V2.1/\beta_{2a}$ channels and found that it enhanced voltage-dependent inactivation and prevented facilitation (Lee et al., 2002), in marked contrast to the effects of VILIP-2 reported here. To complete the comparison of modulation of $Ca_V2.1$ channels by CaBP1 and VILIP-2, we also studied the effects of CaBP1 on $Ca_V2.1/\beta_{1b}$ channels. Under these experimental conditions, coexpression of CaBP1 had no effect on the rate of activation or inactivation of I_{Ca} conducted by $Ca_V2.1/\beta_{1b}$ channels during 1 s depolarizations (Fig. 7*A*) and also had no effect on their voltage dependence of activation (data not shown). Although there was a trend toward increased decay of I_{Ca} during trains of repetitive pulses (Fig. 7*B*), this difference did not reach statistical significance. In contrast to these results for I_{Ca}, replacement of Ca^{2+} with Ba^{2+} eliminates the small effects of Ca^{2+}/CaM-dependent inactivation of $Ca_V2.1/\beta_{1b}$ channels and reveals Ca^{2+}-independent effects of CaBP1. Coexpression of CaBP1 enhanced inactivation of I_{Ba} during single 1 s test pulses (Fig. 7*C*) and during extended trains of depolarizations (Fig. 7*D*). Thus, coexpression of CaBP1 has little effect on I_{Ca} conducted by $Ca_V2.1/\beta_{1b}$ channels but accelerates inactivation of I_{Ba}, opposite to the effect of VILIP-2.

Discussion

Modulation of $Ca_V2.1$ channels by VILIP-2

Our results show that VILIP-2 modulates $Ca_V2.1$ channels in a biphasic manner that depends on the associated β subunit and on Ca^{2+} entry. $Ca_V2.1$ channels with associated β_{2a} subunits have slow voltage-dependent inactivation (Olcese et al., 1994; Chien et al., 1996). VILIP-2 decreases Ca^{2+}/CaM-dependent inactivation of the Ca^{2+} current through $Ca_V2.1/\beta_{2a}$ channels during 1 s depolarizations. Replacing Ca^{2+} with Ba^{2+} as the charge carrier eliminates Ca^{2+}/CaM-dependent inactivation and eliminates the effect of VILIP-2. Similarly, $Ca_V2.1\Delta CBD/\beta_{2a}$ channels, which have impaired CaM binding, do not undergo rapid Ca^{2+}/CaM-dependent inactivation, and inactivation of I_{Ca} is not further slowed by VILIP-2 coexpression. These results are consistent with the conclusion that VILIP-2 occupies the same binding site as endogenous CaM and thereby prevents rapid Ca^{2+}/CaM-dependent inactivation. When bound in place of CaM, VILIP-2 reduces inactivation of $Ca_V2.1/\beta_{2A}$ channels.

Coexpression of VILIP-2 does not alter Ca^{2+}-dependent facilitation of $Ca_V2.1/\beta_{2a}$ channels after a single pulse in paired-pulse facilitation experiments. Evidently, VILIP-2 can bind Ca^{2+} and induce facilitation like CaM. However, the effect of VILIP-2 to slow inactivation allows enhanced facilitation during and after extended trains of depolarizations by reducing cumulative inactivation during the train.

$Ca_V2.1/\beta_{1b}$ channels exhibit rapid voltage-dependent inactivation (De Waard and Campbell, 1995; Hofmann et al., 1999; Lee et al., 2000; Arikkath and Campbell, 2003) and comparatively little acceleration of inactivation by Ca^{2+}/CaM (Lee et al., 1999, 2000). In contrast to $Ca_V2.1/\beta_{2a}$ channels, coexpression of VILIP-2 has no effect on the rapid inactivation of I_{Ca} but slows voltage-dependent inactivation of I_{Ba} to give a rate comparable with inactivation of I_{Ba} through $Ca_V2.1/\beta_{2a}$ channels. Deletion of the CBD blocks the effect of VILIP-2 to slow the rate of inactivation of I_{Ba}, identifying this site as being necessary for VILIP-2 modulation of $Ca_V2.1/\beta_{1b}$. VILIP-2 coexpression also reduces inactivation of I_{Ba} during trains of depolarizations. These results are consistent with the conclusion that VILIP-2 occupies the same binding site as CaM. When bound in place of CaM, VILIP-2 slows inactivation of I_{Ba} but does not enhance facilitation of $Ca_V2.1/\beta_{1b}$ channels during extended trains of depolarizations.

Interaction of VILIP-2 with $Ca_V2.1$ channels

CaM binds to at least two interacting subsites on the carboxyl tail of $Ca_V2.1$, the IQ-like domain and the CBD (Lee et al., 1999, 2003; DeMaria et al., 2001). Sequential Ca^{2+}-dependent interactions with these subsites are required for Ca^{2+}/CaM-dependent facilitation and inactivation (Lee et al., 2003). In contrast, we found that VILIP-2 binds to $Ca_V2.1$ channels at the resting level of Ca^{2+} by interaction with the IQ-like domain and the CBD. VILIP-2 binding was weaker than CaM and was not stable through solubilization and immunoprecipitation; however, covalent cross-linking *in situ* with DSP stabilized this *in vivo* interaction so that it could be measured by solubilization and coimmunoprecipitation. Because mutation of both the IQ-like motif and the CBD were required to prevent binding of VILIP-2, it likely displaces CaM interactions from both of those subsites on $Ca_V2.1$ channels. Evidently, binding of VILIP-2 at resting Ca^{2+} levels and displacement of CaM from the IQ-like domain and the CBD combine to produce the effects that we have recorded in our electrophysiological studies.

Colocalization of VILIP-2 and $Ca_V2.1$ channels in the brain

VILIP-2 is expressed in the neocortex, caudate–putamen, and hippocampus, including both pyramidal neurons and dentate granule cells, and in the Purkinje neurons of the cerebellum (Paterlini et al., 2000). $Ca_V2.1$, β_{2a}, and β_{1b} are also expressed in these regions (Stea et al., 1994; Tanaka et al., 1995; Westenbroek et al., 1995; Sakurai et al., 1996). The $Ca_V2.1/\beta_{2a}$ currents reported here are similar to slowly inactivating P/Q-type Ca^{2+} currents recorded in hippocampal CA1 neurons (Hillyard et al., 1992; Mintz, 1994), cerebellar granule neurons (Randall and Tsien, 1995), and Purkinje neurons (Mintz et al., 1992a,b). Thus, VILIP-2 is present in neurons in which $Ca_V2.1/\beta_{2a}$ is expressed and is therefore able to modulate these channels *in vivo*. Immunocytochemical studies of VILIP-2 localization show broad distribution in the cell bodies and dendrites of hippocampal pyramidal neurons, dentate granule neurons, cortical neurons, and cerebellar Purkinje neurons (Saitoh et al., 1994, 1995). In addition, punctate labeling in the neuropil of the hippocampus and cerebral cortex suggests localization of VILIP-2 in nerve terminals as well (Saitoh et al., 1994, 1995), together with $Ca_V2.1$ channels (Westenbroek et al., 1995). These results indicate that VILIP-2 is colocalized with $Ca_V2.1$ channels in neuronal cell bodies and dendrites and probably in nerve terminals. Our previous results show that CaBP1 and $Ca_V2.1$ channels are colocalized in cell bodies, dendrites, and nerve terminals in the hippocampus and cerebellum (Lee et al., 2002), thereby placing both nCaBPs and $Ca_V2.1$ channels in the same subcellular locations. $Ca_V2.1$ channels in these neuronal subcellular compartments would be modulated in a reciprocal calcium-dependent manner by CaM, CaBP1, and VILIP-2 acting at the same site.

Differential modulation of $Ca_V2.1$ channels by neuronal Ca^{2+}-binding proteins

This study provides new evidence that different Ca^{2+}-binding proteins fine-tune the functional properties of $Ca_V2.1$ channels. Figure 8 illustrates the structural features of CaM, CaBP1, and VILIP-2 and shows their effects on $Ca_V2.1$ channels during single depolarizations and repetitive stimulation as an example of their differential actions. CaM has four EF-hands, which are all functional in binding Ca^{2+}. An α helix connects EF-hands 2 and 3 and divides the molecule into two halves, which function differentially in facilitation and inactivation of $Ca_V2.1$ channels (DeMaria et al., 2001; Lee et al., 2003). High-affinity binding of local Ca^{2+} to EF-hands 3 and 4 initiates facilitation by enhancing interaction with the IQ-like domain, whereas lower-affinity binding of globally increased Ca^{2+} to EF-hands 1 and 2 initiates Ca^{2+}-dependent inactivation by interaction with the CBD (Lee et al., 2000, 2003; DeMaria et al., 2001).

CaBP1 and VILIP-2 have distinct molecular features and functional effects (Fig. 8). EF-hand 2 of CaBP1 has amino acid sequence changes that prevent high-affinity binding of Ca^{2+}, the long N-terminal has a myristoyl lipid anchor, and the central α helix is lengthened by an additional turn compared with CaM (Fig. 8*A*). In contrast, EF-hand 1 of VILIP-2 does not bind Ca^{2+}, the N-terminal is shorter but also has a myristoyl lipid anchor, and the central α helix is similar in length to CaM (Fig. 8*A*). These molecular differences cause different functional effects on $Ca_V2.1$ channels (Fig. 8*B*,*C*). CaM mediates Ca^{2+}-dependent inactivation, CaBP1 causes rapid inactivation regardless of whether Ca^{2+} is the permeant ion, and VILIP-2 causes slow inactivation regardless of whether Ca^{2+} is the permeant ion (Fig. 8*B*). The differences in the effects of these neuronal Ca^{2+}-binding proteins on inactivation during single long depolarizations (Fig. 8*B*) is mir-

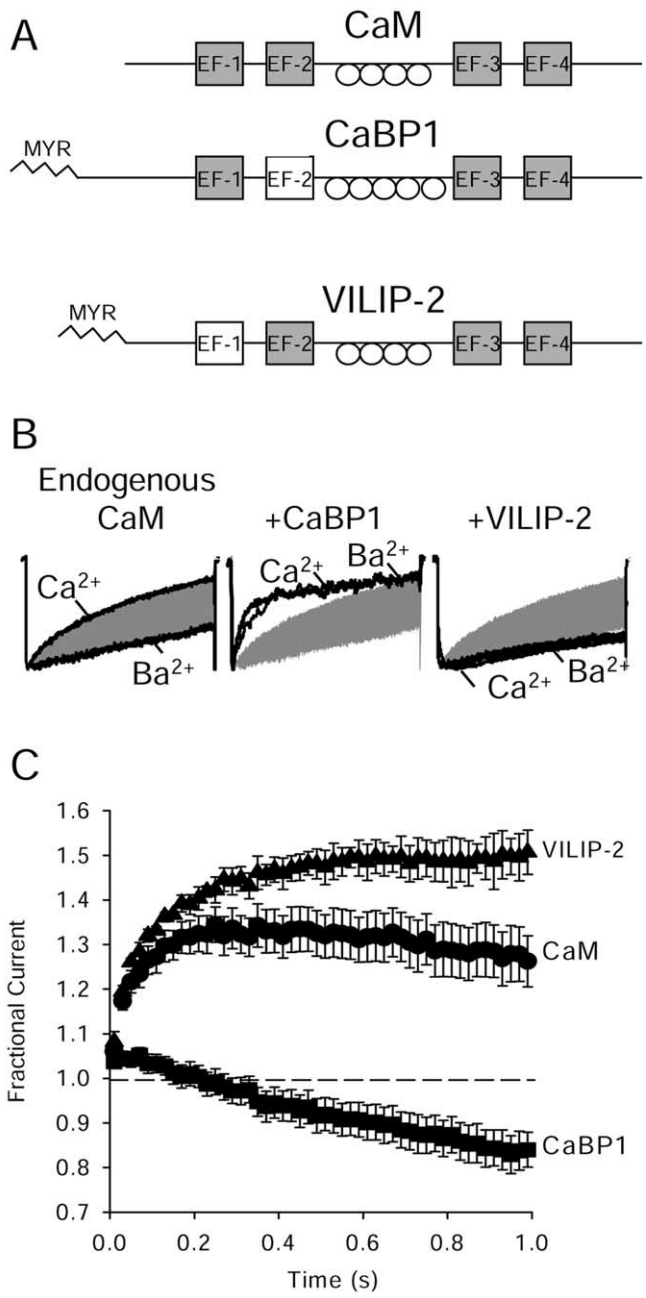

Figure 8. Comparison of the structures and modulatory effects of CaM, VILIP-2, and CaBP1. ***A***, Schematic illustration of the structures of CaM, CaBP1, and VILIP-2. EF-hands that are active in binding Ca^{2+} are indicated in gray, and inactive EF-hands are indicated in white. Circles denote the central α helix connecting EF-hands 2 and 3. Bent lines indicate N-terminal myristoylation. The lengths of the line segments approximately correspond to the length of the amino acid sequences. ***B***, Ca^{2+}-dependent inactivation of $Ca_V2.1/\beta_{2a}$ channels with CaM, CaBP1, or VILIP-2. Overlapped Ca^{2+} and Ba^{2+} currents are plotted. The shaded area indicates the Ca^{2+}-dependent increase in inactivation caused by CaM. ***C***, Ca^{2+}-dependent facilitation and inactivation of $Ca_V2.1/\beta_{2a}$ channels with CaM, CaBP1, or VILIP-2. The CaM and CaBP1 data in ***B*** and ***C*** were modified from Lee et al. (2000) and (2002), respectively. Error bars represent SEM.

rored in their effects on facilitation and inactivation during trains of stimuli (Fig. 8*C*). CaM causes facilitation followed by inactivation, VILIP-2 causes only enhanced facilitation, and CaBP1 causes only enhanced inactivation. These differential effects on presynaptic Ca^{2+} channels would alter the encoding properties of the presynaptic terminal by changing its response to repetitive stimuli from facilitation followed by inactivation to either facilitation only or inactivation only (Fig. 8). Thus, in nerve terminals where these Ca^{2+}-binding proteins are colocalized with $Ca_V2.1$ channels, the input-output relationships of the corresponding synapses would be influenced in an important way by regulation of the presynaptic Ca^{2+} channels by differentially expressed neurospecific Ca^{2+}-binding proteins.

References

Ames JB, Ishima R, Tanaka T, Gordon JI, Stryer L, Ikura M (1997) Molecular mechanics of calcium-myristoyl switches. Nature 389:198–202.

Arikkath J, Campbell KP (2003) Auxiliary subunits: essential components of the voltage-gated calcium channel complex. Curr Opin Neurobiol 13:298–307.

Bernstein HG, Baumann B, Danos P, Diekmann S, Bogerts B, Gundelfinger ED, Braunewell KH (1999) Regional and cellular distribution of neural visinin-like protein immunoreactivities (VILIP-1 and VILIP-3) in human brain. J Neurocytol 28:655–662.

Bernstein HG, Becker A, Keilhoff G, Spilker C, Gorczyca WA, Braunewell KH, Grecksch G (2003) Brain region-specific changes in the expression of calcium sensor proteins after repeated applications of ketamine to rats. Neurosci Lett 339:95–98.

Burgess DL, Biddlecome GH, McDonough SI, Diaz ME, Zilinski CA, Bean BP, Campbell KP, Noebels JL (1999) Beta subunit reshuffling modifies N- and P/Q-type Ca^{2+} channel subunit compositions in lethargic mouse brain. Mol Cell Neurosci 13:293–311.

Burgoyne RD, Weiss JL (2001) The neuronal calcium sensor family of calcium-binding proteins. Biochem J 353:1–12.

Chien AJ, Carr KM, Shirokov RE, Rios E, Hosey MM (1996) Identification of palmitoylation sites within the L-type calcium channel β_{2a} subunit and effects on channel function. J Biol Chem 271:26465–26468.

De Castro E, Nef S, Fiumelli H, Lenz SE, Kawamura S, Nef P (1995) Regulation of rhodopsin phosphorylation by a family of neuronal calcium sensors. Biochem Biophys Res Commun 216:133–140.

DeMaria CD, Soong TW, Alseikhan BA, Alvania RS, Yue DT (2001) Calmodulin bifurcates the local Ca^{2+} signal that modulates P/Q-type Ca^{2+} channels. Nature 411:484–489.

De Waard M, Campbell KP (1995) Subunit regulation of the neuronal α_{1A} Ca^{2+} channel expressed in *Xenopus* oocytes. J Physiol (Lond) 485:619–634.

Dodge Jr FA, Rahamimoff R (1967) Co-operative action of calcium ions in transmitter release at the neuromuscular junction. J Physiol (Lond) 193:419–432.

Ellis SB, Williams ME, Ways NR, Brenner R, Sharp AH, Leung AT, Campbell KP, McKenna E, Koch WJ, Hui A, Schwartz A, Harpold MM (1988) Sequence and expression of mRNAs encoding the alpha 1 and alpha 2 subunits of a DHP-sensitive calcium channel. Science 241:1661–1664.

Erickson MG, Liang H, Mori MX, Yue DT (2003) FRET two-hybrid mapping reveals function and location of L-type calcium channel CaM preassociation. Neuron 39:97–107.

Haeseleer F, Sokal I, Verlinde CL, Erdjument-Bromage H, Tempst P, Pronin AN, Benovic JL, Fariss RN, Palczewski K (2000) Five members of a novel calcium-binding protein (CaBP) subfamily with similarity to calmodulin. J Biol Chem 275:1247–1260.

Hamashima H, Tamaru T, Noguchi H, Kobayashi M, Takamatsu K (2001) Immunochemical assessment of neural visinin-like calcium-binding protein 3 expression in rat brain. Neurosci Res 39:133–143.

Herlitze S, Garcia DE, Mackie K, Hille B, Scheuer T, Catterall WA (1996) Modulation of Ca^{2+} channels by G protein $\beta\gamma$ subunits. Nature 380:258–262.

Hillyard DR, Monje VD, Mintz IM, Bean BP, Nadasdi L, Ramachandran J, Miljanich G, Azimi-Zoonooz A, McIntosh JM, Cruz LJ, et al. (1992) A new Conus peptide ligand for mammalian presynaptic Ca^{2+} channels. Neuron 9:69–77.

Hofmann F, Lacinová L, Klugbauer N (1999) Voltage-dependent calcium channels: from structure to function. Rev Physiol Biochem Pharmacol 139:33–87.

Ikeda SR (1996) Voltage-dependent modulation of N-type calcium channels by G-protein $\beta\gamma$ subunits. Nature 380:255–258.

Lee A, Wong ST, Gallagher D, Li B, Storm DR, Scheuer T, Catterall WA (1999) Ca^{2+}/calmodulin binds to and modulates P/Q-type calcium channels. Nature 399:155–159.

Lee A, Scheuer T, Catterall WA (2000) Ca^{2+}-calmodulin dependent inactivation and facilitation of P/Q-type Ca^{2+} channels. J Neurosci 20:6830–6838.

Lee A, Westenbroek RE, Haeseleer F, Palczewski K, Scheuer T, Catterall WA (2002) Differential modulation of $Ca_V2.1$ channels by calmodulin and Ca^{2+}-binding protein 1. Nat Neurosci 5:210–217.

Lee A, Zhou H, Scheuer T, Catterall WA (2003) Molecular determinants of calcium/calmodulin-dependent regulation of $Ca_V2.1$ channels. Proc Natl Acad Sci USA 100:16059–16064.

Lenz SE, Henschel Y, Zopf D, Voss B, Gundelfinger ED (1992) VILIP, a cognate protein of the retinal calcium binding proteins visinin and recoverin, is expressed in the developing chicken brain. Brain Res Mol Brain Res 15:133–140.

Llinás R, Sugimori M, Lin JW, Cherksey B (1989) Blocking and isolation of a calcium channel from neurons in mammals and cephalopods utilizing a toxin fraction (FTX) from funnel-web spider poison. Proc Natl Acad Sci USA 86:1689–1693.

Ludwig A, Flockerzi V, Hofmann F (1997) Regional expression and cellular localization of the α_1 and β subunit of high voltage-activated calcium channels in rat brain. J Neurosci 17:1339–1349.

Mintz IM (1994) Block of calcium channels in rat central neurons by the spider toxin ω-Aga-IIIA. J Neurosci 14:2844–2853.

Mintz IM, Venema VJ, Swiderek KM, Lee TD, Bean BP, Adams ME (1992a) P-type calcium channels blocked by the spider toxin omega-Aga-IVA. Nature 355:827–829.

Mintz IM, Adams ME, Bean BP (1992b) P-type calcium channels in rat central and peripheral neurons. Neuron 9:85–95.

Mintz IM, Sabatini BL, Regehr WG (1995) Calcium control of transmitter release at a cerebellar synapse. Neuron 15:675–688.

Olcese R, Qin N, Schneider T, Neely A, Wei X, Stefani E, Birnbaumer L (1994) The amino terminus of a calcium channel beta subunit sets rates of channel inactivation independently of the subunit's effect on activation. Neuron 13:1433–1438.

Pate P, Mochca-Morales J, Wu Y, Zhang JZ, Rodney GG, Serysheva II, Williams BY, Anderson ME, Hamilton SL (2000) Determinants for calmodulin binding on voltage-dependent Ca^{2+} channels. J Biol Chem 275:39786–39792.

Paterlini M, Revilla V, Grant AL, Wisden W (2000) Expression of the neuronal calcium sensor protein family in the rat brain. Neuroscience 99:205–216.

Perez-Reyes E, Castellano A, Kim HS, Bertrand P, Baggstrom E, Lacerda AE, Wei X, Birnbaumer L (1992) Cloning and expression of a cardiac/brain β subunit of the L-type calcium channel. J Biol Chem 267:1792–1797.

Randall A, Tsien RW (1995) Pharmacological dissection of multiple types of Ca^{2+} channel currents in rat cerebellar granule neurons. J Neurosci 15:2995–3012.

Regehr WG, Mintz IM (1994) Participation of multiple calcium channel types in transmission at single climbing fiber to Purkinje cell synapses. Neuron 12:605–613.

Saitoh S, Takamatsu K, Kobayashi M, Noguchi T (1994) Immunohistochemical localization of neural visin-like calcium binding protein-2. Neurosci Lett 171:155–158.

Saitoh S, Kobayashi M, Kuroki T, Noguchi T, Takamatsu K (1995) The development of neural visinin-like calcium-binding protein-2 immunoreactivity in the rat neocortex and hippocampus. Neurosci Res 23:383–388.

Sakurai T, Westenbroek RE, Rettig J, Hell J, Catterall WA (1996) Biochemical properties and subcellular distribution of the BI and rbA isoforms of α_{1A} subunits of brain calcium channels. J Cell Biol 134:511–528.

Sallese M, Iacovelli L, Cumashi A, Capobianco L, Cuomo L, De Blasi A (2000) Regulation of G protein-coupled receptor kinase subtypes by calcium sensor proteins. Biochim Biophys Acta 1498:112–121.

Spilker C, Dresbach T, Braunewell KH (2002) Reversible translocation and activity-dependent localization of the calcium-myristoyl switch protein VILIP-1 to different membrane compartments in living hippocampal neurons. J Neurosci 22:7331–7339.

Starr TVB, Prystay W, Snutch TP (1991) Primary structure of a calcium channel that is highly expressed in the rat cerebellum. Proc Natl Acad Sci USA 88:5621–5625.

Stea A, Tomlinson WJ, Soong TW, Bourinet E, Dubel SJ, Vincent SR, Snutch TP (1994) The localization and functional properties of a rat brain α_{1A} calcium channel reflect similarities to neuronal Q- and P-type channels. Proc Natl Acad Sci USA 91:10576–10580.

Takahashi T, Momiyama A (1993) Different types of calcium channels mediate central synaptic transmission. Nature 366:156–158.

Tanaka O, Sakagami H, Kondo H (1995) Localization of mRNAs of voltage-dependent Ca^{2+}-channels: four subtypes of α1- and β-subunits in developing and mature rat brain. Mol Brain Res 30:1–16.

Westenbroek RE, Sakurai T, Elliott EM, Hell JW, Starr TVB, Snutch TP, Catterall WA (1995) Immunochemical identification and subcellular distribution of the α_{1A} subunits of brain calcium channels. J Neurosci 15:6403–6418.

Wheeler DB, Randall A, Tsien RW (1994) Roles of N-type and Q-type Ca^{2+} channels in supporting hippocampal synaptic transmission. Science 264:107–111.

Wu LG, Westenbroek RE, Borst JG, Catterall WA, Sakmann B (1999) Calcium channel types with distinct presynaptic localization couple differentially to transmitter release in single calyx-type synapses. J Neurosci 19:726–736.

Zucker RS, Regehr WG (2002) Short-term synaptic plasticity. Annu Rev Physiol 64:355–405.